Chirality of matter shows up via spin excitations

S. Bordács, I. Kézsmárki, D. Szaller, L. Demkó, N. Kida, H. Murakawa, Y. Onose,

R. Shimano, T. Rõõm, U. Nagel, S. Miyahara, N. Furukawa, Y. Tokura

I. Calculation of optical properties in simultaneously chiral and magnetic materials.

When a chiral crystal is placed in magnetic field, besides natural and magnetic circular dichroism (NCD and MCD, respectively), a new magneto-optical effect, the so-called magneto-chiral dichroism (MChD) can arise. Among the possible systems exhibiting the MChD effect, the highest symmetry ones are chiral crystals with the 432 cubic point group placed in a magnetic field pointing along one of their principal axes. First, we study this situation, i.e. when the magnetic point symmetry is $42'2'$ where $'$ means the time-reversal operation. In this case the number of the independent elements in the relevant optical property tensors ($\hat{\epsilon}$, $\hat{\mu}$, $\hat{\chi}^{me}$ and $\hat{\chi}^{em}$) is reduced and the optical phenomena can be more easily deduced than in the $22'2'$ point symmetry of $Ba_2CoGe_2O_7$ in its chiral state. Next, we turn to the description of the spin Hamiltonian used to reproduce the multiferroic ground state of $Ba_2CoGe_2O_7$ and to evaluate the optical response functions. Finally, we derive approximate expressions describing NCD and MChD effect in the actual symmetry of $Ba_2CoGe_2O_7$.

In the long-wavelength region of light, NCD, MCD, and MChD can be phenomenologically described by the Maxwell's equations

$$\omega \mathbf{B}^\omega = \mathbf{k} \times \mathbf{E}^\omega, \tag{1}$$

$$-\omega \mathbf{D}^\omega = \mathbf{k} \times \mathbf{H}^\omega, \tag{2}$$

if dynamical magnetoelectric effects are introduced via

$$\mathbf{B}^\omega = \hat{\mu}\mu_0 \mathbf{H}^\omega + \hat{\chi}^{me}\sqrt{\epsilon_0\mu_0}\mathbf{E}^\omega, \tag{3}$$

$$\mathbf{D}^\omega = \hat{\epsilon}\epsilon_0 \mathbf{E}^\omega + \hat{\chi}^{em}\sqrt{\epsilon_0\mu_0}\mathbf{H}^\omega, \tag{4}$$

besides the usual dielectric permittivity and magnetic permeability[1]. According to Neumann's principle, in the $42'2'$ symmetry the dynamical susceptibility tensors have the following form:

$$\hat{\mu}(\omega) = \begin{pmatrix} \mu_{xx} & 0 & \mu_{xz} \\ 0 & \mu_{yy} & 0 \\ -\mu_{xz} & 0 & \mu_{xx} \end{pmatrix}, \quad \hat{\epsilon}(\omega) = \begin{pmatrix} \epsilon_{xx} & 0 & \epsilon_{xz} \\ 0 & \epsilon_{yy} & 0 \\ -\epsilon_{xz} & 0 & \epsilon_{xx} \end{pmatrix}, \tag{5}$$

$$\hat{\chi}^{\mathrm{me}}(\omega) = \begin{pmatrix} \chi_{xx}^{\mathrm{me}} & 0 & \chi_{xz}^{\mathrm{me}} \\ 0 & \chi_{yy}^{\mathrm{me}} & 0 \\ -\chi_{xz}^{\mathrm{me}} & 0 & \chi_{xx}^{\mathrm{me}} \end{pmatrix}, \quad \hat{\chi}^{\mathrm{em}}(\omega) = \begin{pmatrix} -\chi_{xx}^{\mathrm{me}} & 0 & -\chi_{xz}^{\mathrm{me}} \\ 0 & -\chi_{yy}^{\mathrm{me}} & 0 \\ \chi_{xz}^{\mathrm{me}} & 0 & -\chi_{xx}^{\mathrm{me}} \end{pmatrix}, \tag{6}$$

when the principal axes point along the x, y and z directions, and $\mathbf{B}_{dc} \| \mathrm{y}$. The diagonal terms are even function of the magnetic field, while the off-diagonal components change sign when the direction of the field is reversed.

The complex refractive index, $N = ck/\omega$, can be calculated from the Maxwell equations, Eqs. (1) and (2). For magnetic fields parallel to the propagation direction, $\mathbf{B}_{dc} \| \mathbf{k}$, one obtains

$$N^{\pm} = \sqrt{(\epsilon_{xx} \mp i\epsilon_{xz})(\mu_{xx} \mp i\mu_{xz})} \mp is_k \chi_{xx}^{\mathrm{me}} - s_k \chi_{xz}^{\mathrm{me}} \tag{7a}$$

$$\approx \sqrt{\epsilon_{xx}\mu_{xx}} \mp i\frac{\epsilon_{xz}\mu_{xx} + \epsilon_{xx}\mu_{xz}}{\sqrt{\epsilon_{xx}\mu_{zz}}} \mp is_k \chi_{xx}^{\mathrm{me}} - s_k \chi_{xz}^{\mathrm{me}}. \tag{7b}$$

The eigenmodes correspond to the two circularly polarized states, $\mathbf{E}_{\pm}^{\omega} \propto (\mathbf{e}_x \mp i\mathbf{e}_z)$. Please note that beside the polarization state, $N^{\pm}$ depend on the sign of the propagation direction, $s_k = k_y/|k_y|$. Correspondingly, each of the four eigenmodes, the left- and right-handed beams propagating along $\mathbf{k}$ and $-\mathbf{k}$ directions, have different refractive indices.

In the experiments the power absorption, the polarization rotation and ellipticity were measured for initially linearly polarized light transmitted trough the sample. If the sample is thin (the intensity losses for both circular polarizations are small compared to the intensity of the incident light beam) the absorption coefficient can be approximated as:

$$\alpha(s_k) = 2\frac{\omega}{c}\mathrm{Im}\left[\frac{N^{+}(s_k) + N^{-}(s_k)}{2}\right], \tag{8}$$

and the complex polarization rotation for unit length as:

$$\Phi(s_k) = \theta(s_k) + i\eta(s_k) = -\frac{\omega}{c}\frac{N^{+}(s_k) - N^{-}(s_k)}{2}. \tag{9}$$

The magneto-chiral effect is defined as the non-reciprocal part of the absorption coefficient:

$$\alpha(s_k = +1) - \alpha(s_k = -1) = -4\frac{\omega}{c}\text{Im}\left[\chi_{xz}^{\text{me}}\right]. \tag{10}$$

Therefore, the magnetic field-odd off-diagonal components of the magnetoelectric tensor are responsible for the MChD. (These elements are odd both in time-reversal and spatial inversion.) Using Eq. (7b) and (9), MCD and NCD are obtained as

$$\{\Phi(s_k = +1) + \Phi(s_k = -1)\}/2 \approx i\frac{\omega}{c}\frac{\epsilon_{xz}\mu_{xx} + \epsilon_{xx}\mu_{xz}}{\sqrt{\epsilon_{xx}\mu_{zz}}}, \tag{11}$$

$$\{\Phi(s_k = +1) - \Phi(s_k = -1)\}/2 = i\frac{\omega}{c}\chi_{xx}^{\text{me}}, \tag{12}$$

respectively. In this approximation, the second, third and fourth terms in Eq. (7b), the circular anisotropy terms, correspond to the MCD, the NCD and the MChD effect. The first term describe the usual case without such anisotropies. As is clear from the previous example, the dynamical magnetoelectric effect is indispensable in the description of the optical activity and the MChD effect.

Chirality arises in $Ba_2CoGe_2O_7$ with non-centrosymmetric lattice structure when magnetic field is applied along the [100] or [010] direction and all the mirror-plane symmetries are broken. Below T_N=6.7 K, a simple two-sublattice antiferromagnetic order is realized and the optical properties are probed for the excitation of this ground state. The magnetoelectric effect comes from the interplay between the spin-orbit coupling acting on the S=3/2 spins of the Co^{2+} ions and the underlying non-centrosymmetric crystal structure[2]. The magnetic ground state is well reproduced by the following spin Hamiltonian under external magnetic field:

$$\mathcal{H} = \sum_{n.n.}\{J\mathbf{S}_i \cdot \mathbf{S}_j - D_{ij}^z(S_i^x S_j^y - S_i^y S_j^x)\} + \sum\{\Lambda(S_i^z)^2 - g\mu_B\mathbf{B}_{dc} \cdot \mathbf{S}_i\}. \tag{13}$$

Here J describes the isotropic term of the spin exchange coupling, D_{ij}^z is the Dzyaloshinsky-Moriya interaction, and Λ corresponds to the uniaxial single-ion anisotropy. The parameters for $Ba_2CoGe_2O_7$ are estimated as $J = 0.175$ meV, $D_z = 7 \times 10^{-3}$ meV, $\Lambda = 1.4$ meV, and $g = 2.1$. Using the spin structure of the canted antiferromagnetic ground state, the spin-dependent electric polarization is captured via a metal-ligand hybridization mechanism on

the CoO$_4$ tetrahedra

$$\mathbf{p}_i = \begin{pmatrix} -K \left[\cos(2\kappa_i)(S_i^z S_i^x + S_i^x S_i^z) + \sin(2\kappa_i)(S_i^y S_i^z + S_i^z S_i^y)\right] \\ K \left[\cos(2\kappa_i)(S_i^y S_i^z + S_i^z S_i^y) + \sin(2\kappa_i)(S_i^z S_i^x + S_i^x S_i^z)\right] \\ K \left[\cos(2\kappa_i)\{(S_i^y)^2 - (S_i^x)^2\} - \sin(2\kappa_i)(S_i^x S_i^y + S_i^y S_i^x)\right] \end{pmatrix}, \qquad (14)$$

where $\mathbf{p}_i$ is the electric polarization on the i-th CoO$_4$ tetrahedron. The strength of the magnetoelectric coupling parameter is $K = 4.6 \times 10^{-32}$ C·m [3]. We emphasize here that both the dc and ac magnetoelectric properties are obtained with these values and no adjustment of the parameters was done while calculating the dynamical susceptibilities.

Dynamical susceptibility tensors, $\hat{\mu}$, $\hat{\epsilon}$, $\hat{\chi}^{me}$ and $\hat{\chi}^{em}$ are calculated from the Kubo formula treating only the excitations of the ground state. Their components are defined as

$$\mu_{\gamma\kappa}(\omega) = \delta_{\gamma\kappa} + \frac{2\mu_0}{\hbar NV}\sum_n \frac{\omega_{no}\Re\{\langle 0|M_\gamma|n\rangle\langle n|M_\kappa|0\rangle\} + i\omega\Im\{\langle 0|M_\gamma|n\rangle\langle n|M_\kappa|0\rangle\}}{\omega_{no}^2 - \omega^2 - 2i\omega\delta}, \quad (15)$$

$$\epsilon_{\gamma\kappa}(\omega) = \epsilon_\gamma^\infty \delta_{\gamma\kappa} + \frac{2}{\hbar NV\epsilon_0}\sum_n \frac{\omega_{no}\Re\{\langle 0|P_\gamma|n\rangle\langle n|P_\kappa|0\rangle\} + i\omega\Im\{\langle 0|P_\gamma|n\rangle\langle n|P_\kappa|0\rangle\}}{\omega_{no}^2 - \omega^2 - 2i\omega\delta}, \quad (16)$$

$$\chi_{\gamma\kappa}^{\text{me}}(\omega) = \frac{2}{\hbar NV}\sqrt{\frac{\mu_0}{\epsilon_0}}\sum_n \frac{\omega_{no}\Re\{\langle 0|M_\gamma|n\rangle\langle n|P_\kappa|0\rangle\} + i\omega\Im\{\langle 0|M_\gamma|n\rangle\langle n|P_\kappa|0\rangle\}}{\omega_{no}^2 - \omega^2 - 2i\omega\delta}, \quad (17)$$

$$\chi_{\gamma\kappa}^{\text{em}}(\omega) = \frac{2}{\hbar NV}\sqrt{\frac{\mu_0}{\epsilon_0}}\sum_n \frac{\omega_{no}\Re\{\langle 0|P_\gamma|n\rangle\langle n|M_\kappa|0\rangle\} + i\omega\Im\{\langle 0|P_\gamma|n\rangle\langle n|M_\kappa|0\rangle\}}{\omega_{no}^2 - \omega^2 - 2i\omega\delta}, \quad (18)$$

where $\mathbf{M} = \sum_i g\mu_B \mathbf{S}_i$ and $\mathbf{P} = \sum_i \mathbf{p}_i$. Here, $|0\rangle$ is the ground state, $|n\rangle$ are the excited states of the spin system, and $\hbar\omega_{n0}$ are excitation energies from the ground state to $|n\rangle$ while $\gamma, \kappa = x, y$, and z. N is the total number of spins and V is the volume of the system. Terms associated with the real ($\Re$) / imaginary ($\Im$) part of the transition matrix elements are noted as $'$ / $''$ and change sign / remain invariant under time reversal, respectively. The two cross-effects are related by the Kubo formula according to $\chi_{\gamma\kappa}^{\text{me}}(\omega) = \chi'_{\gamma\kappa}(\omega) + \chi''_{\gamma\kappa}(\omega)$ and $\chi_{\gamma\kappa}^{\text{em}}(\omega) = \chi'_{\kappa\gamma}(\omega) - \chi''_{\kappa\gamma}(\omega)$. Please note that in insulating materials in the dc limit ($\omega = 0$) all the above susceptibilities are purely real and correspondingly $\chi_{\gamma\kappa}^{\text{me}}(0) = \chi_{\kappa\gamma}^{\text{em}}(0)$. Under $\mathbf{B}_{dc}\|[010]\|y$, the susceptibilities (15)-(18) for the Hamiltonian (13) are directly calculated on N-site clusters ($N = 8, 10$, and 12) by Lanczos methods, where the Dirac-δ functions in the frequency dependence of the susceptibilities are replaced by Lorentzian of $\epsilon/\Lambda = 0.05$

width. The non-zero components of the tensors are found to be

$$\hat{\mu}(\omega) = \begin{pmatrix} \mu_{xx} & 0 & \mu_{xz} \\ 0 & \mu_{yy} & 0 \\ -\mu_{xz} & 0 & \mu_{zz} \end{pmatrix}, \quad \hat{\epsilon}(\omega) = \begin{pmatrix} \epsilon_{xx} & 0 & \epsilon_{xz} \\ 0 & \epsilon_{yy} & 0 \\ -\epsilon_{xz} & 0 & \epsilon_{xz} \end{pmatrix} \quad (19)$$

$$\hat{\chi}^{\mathrm{me}}(\omega) = \begin{pmatrix} \chi^{\mathrm{me}}_{xx} & 0 & \chi^{\mathrm{me}}_{xz} \\ 0 & \chi^{\mathrm{me}}_{yy} & 0 \\ \chi^{\mathrm{me}}_{zx} & 0 & \chi^{\mathrm{me}}_{zz} \end{pmatrix}, \quad \hat{\chi}^{\mathrm{em}}(\omega) = \begin{pmatrix} -\chi^{\mathrm{me}}_{xx} & 0 & \chi^{\mathrm{me}}_{zx} \\ 0 & -\chi^{\mathrm{me}}_{yy} & 0 \\ \chi^{\mathrm{me}}_{xz} & 0 & -\chi^{\mathrm{me}}_{zz} \end{pmatrix}, \quad (20)$$

which are consistent with the forms determined from the $2'22'$ magnetic point group of the magnetically ordered state in $\mathbf{B}_{dc} \parallel [010]$. The diagonal terms are again even functions of the magnetic field, while the off-diagonal components change sign when the direction of the field is reversed. We emphasize that all of the symmetry allowed tensor elements are non-zero, including the components of the dielectric permittivity (16) and the dynamical magnetoelectric tensors (17) and (18), which is the consequence of the strong coupling between the spins and the local electric dipoles. In the present approach optical properties are discussed in terms of second ranked tensors (the dielectric permittivity, the magnetic permeability, and the magnetoelectric tensors). These microscopic response functions describe all the linear optical effects in the long-wavelength limit. The lattice structure and the magnetic order together specify the magnetic point group in the ground state and, thus, determine the symmetry of the optical properties as well. In this description the effect of the dc magnetic field is taken into account through the change of the magnetic point group. This scheme generally captures the linear optical properties.

Due to the low symmetry of the system, solution of the Maxwell's equations (1) and (2) is not as straight forward as in the $42'2'$ point group studied previously. Instead we derive approximated formulas in the thin sample limit. First, let us consider a light beam propagating to z-direction, i.e. $\mathbf{k} \parallel [001]$. Thus, the so-called Voigt geometry is realized with $\mathbf{k} \perp \mathbf{B}_{dc}$. When such a beam with linear polarization (e.g. $E_\omega \parallel \mathrm{y}$ and $H_\omega \parallel \mathrm{x}$) enters into the matter, the absorption coefficient is mainly determined by the diagonal components of the dielectric permittivity and the magnetic permeability tensors:

$$\alpha \approx \frac{2\omega}{c} \mathrm{Im} \left[\sqrt{\epsilon_{yy} \mu_{xx}} \right]. \quad (21)$$

The isotropy of the plane is broken due to the presence of $\mathbf{B}_{dc} \parallel [010]$. On one hand, this induces linear birefringence and dichroism correspondingly $\epsilon_{xx} \neq \epsilon_{yy}$ and $\mu_{xx} \neq \mu_{yy}$.

5

However, if the polarization of the incident light is set parallel to the principal axes, the polarization state is preserved. On the other hand, the diagonal components of the $\hat{\chi}^{me}$ and $\hat{\chi}^{em}$ magnetoelectric tensors cause circular anisotropy, which rotates the polarization and generally makes it elliptical. The complex polarization rotation $\Phi = \theta + i\eta$, is derived as [4]

$$\Phi(s_k) \approx i s_k \frac{\omega}{c} \frac{\chi_{xx}^{me} + \chi_{yy}^{me}}{2}. \tag{22}$$

Φ changes sign between forward and backward propagation, thus it is related to the NCD effect in the field induced chiral state of the material. The condition $\mathbf{k} \perp \mathbf{B}_{dc}$ and the fact that χ_{xx}^{me} and χ_{yy}^{me} are even function of $\mathbf{B}_{dc}$ clearly exclude the onset of either MCD or MChD. Theoretical curves in Fig. 3a are calculated using Eqs. (21) and (22). We note that in few non-chiral crystals circular dichroism can arise in specific directions[1]. Though the paramagnetic state of $Ba_2CoGe_2O_7$ belongs to this class, circular dichroism for light propagation along the [001] direction ($\overline{4}$ axis) is not allowed by its point symmetry $\overline{4}2m$, thus the observed NCD effect purely originates from the magnetically induced chirality of the material.

In Faraday geometry when $\mathbf{k} \| \mathbf{B}_{dc} \| [010]$, the absorption and the MChD are calculated as:

$$\alpha(s_k) \approx \frac{2\omega}{c} \text{Im} \left[\sqrt{\epsilon_{xx} \mu_{zz}} - s_k \chi_{xz}^{me} \right], \tag{23}$$

$$\Delta\alpha = \alpha(s_k = +1) - \alpha(s_k = -1) = \frac{4\omega}{c} \text{Im} \left[\chi_{xz}^{me} \right], \tag{24}$$

respectively. In Eqs. (23) and (24) the incident light polarization is $\mathbf{E}^\omega \| x$. The absorption coefficient is the function of the propagation direction, s_k, i.e. the absorbed intensity is different for counterpropagating light beams. Since the χ_{xz}^{me} element of the magnetoelectric tensor has odd parity under the time reversal operation, its sign can be changed by the reversal of the field direction as demonstrated in the experiment. Theoretical curves in Fig. 4c-d are calculated using Eqs. (23) and (24).

Using $\hat{\mu}$, $\hat{\epsilon}$, $\hat{\chi}^{me}$ and $\hat{\chi}^{em}$ obtained from Eqs. (15)-(18), the absorption coefficient $\alpha(\omega)$, polarization $\theta(\omega)$, and ellipticity $\eta(\omega)$ can be obtained for any light polarizations according to Eqs. (21)-(24). As shown in Fig. 3a and Figs. 4c-d, the absorption, the complex polarization rotation and the MChD spectra observed in the experiments are reproduced well by the numerical calculations.

The NCD and gyrotropy spectra measured over the range of the spin excitations in the field-induced chiral state of $Ba_2CoGe_2O_7$ ($\mathbf{B}_{dc} \| [010]$) for various propagation directions

and polarization configurations is shown in Fig. S1. The optical activity is larger for the 1 THz resonance with strong magnetoelectric nature, except for the $\mathbf{E}_\omega\|[001]$ $\mathbf{B}_\omega\|\mathbf{B}_{dc}\|[010]$ configuration when it shows up only for 0.5 THz mode of mostly magnetic dipole character. The large ellipticity values indicate that the initially linearly polarized light would become fully circularly polarized after passing through samples with thickness of few mm. We note here that, due to the additional linear birefringence/dichroism effects introduced by the tetragonal symmetry of the compound or induced by the external magnetic field, in reality the polarization eigenstates of light are elliptically polarized.
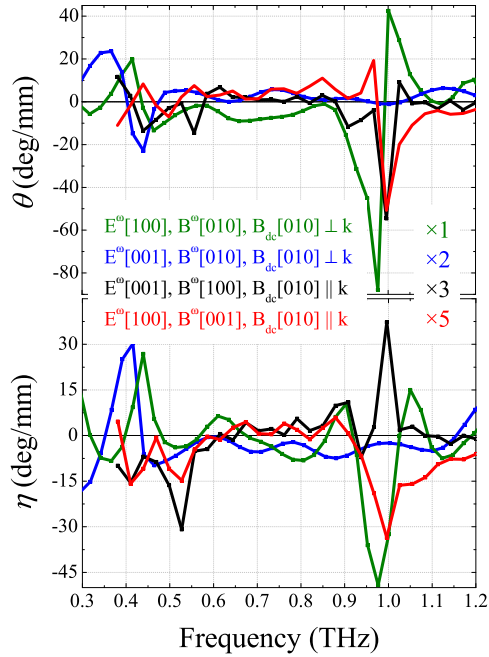

FIG. S1: | **Polarization rotation, θ, and ellipticity, η, spectra in the field-induced chiral state of $Ba_2CoGe_2O_7$ for several polarization configurations.** Outside the two spin resonances at about 0.5 THz and 1 THz both the polarization rotation and ellipticity signal vanish, excluding possible contributions from the linear birefringence and dichroism due to a misalignment between the polarization of the incident light and the optical axes of the crystal. The NCD and the gyrotropy is larger for the 1 THz resonance except for the $\mathbf{E}_\omega\|[001]$ $\mathbf{B}_\omega\|\mathbf{B}_{dc}\|[010]$ case when only the 0.5 THz magnon modes shows appreciable effect.

II. Polarization analysis in time-domain THz spectroscopy.

We adopted the terahertz (THz) time-domain spectroscopy to obtain the complex transmission spectrum in the frequency range of $0.2 - 2\,\text{THz}$ with a resolution of $0.05\,\text{THz}$.
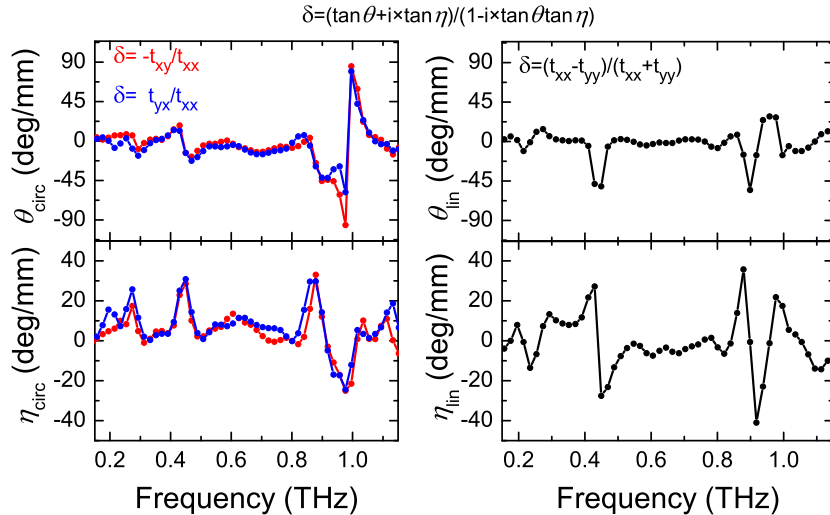

FIG. S2: | **Polarization rotation, θ, and ellipticity, η, spectra in the field-induced chiral state of $\text{Ba}_2\text{CoGe}_2\text{O}_7$ with $\mathbf{B}_{dc} = 7\,\mathbf{T}$ parallel to [010].** The spectra in the left and right panel are the anisotropies related to the off-diagonal and diagonal components of the 2×2 complex Jones matrix.

We carried out time-domain transmission experiments in several polarization configurations and determined each complex element of the 2×2 $\hat{t}_{ij}$ transmission matrix. This procedure was done for $\mathbf{B}_{dc} \parallel$ [100] and [010]. For propagation along [001], we found that the off-diagonal part of the transmission matrix is antisymmetric in the $\mathbf{x}$=[100], $\mathbf{y}$=[010] frame with contributions from circular anisotropy as seen in the left panel of Fig. S2. For most of the modes, the diagonal elements are different due to the magnetic field induced linear anisotropy with optical axes parallel and perpendicular to the field as clear from the right panel of Fig. S2. Please note that xy-plane is isotropic in the paramagnetic phase due to $\overline{4}$ operation around the [001] axis. Under these conditions, light beams with initial linear polarization either parallel or perpendicular to $\mathbf{B}_{dc}$ would experience polarization changes solely due to circular birefringence and dichroism as long as θ and η are small. In this thin sample limit, the $\Phi_{circ} = \theta_{circ} + i\eta_{circ}$ (left panel of Fig. S2) and $\Phi_{lin} = \theta_{lin} + i\eta_{lin}$ (right panel of Fig. S2) purely comes from circular and linear anisotropy, respectively.

We show that even in the thick sample limit, relevant to the present case, the ratio Φ_{circ}/Φ_{lin} corresponds to the relative strength of the contributions from circular and linear anisotropy in the complex refractive index. In the presence of circular and linear optical anisotropy the transmission matrix has the following form[5]:

$$\hat{t}_{ij} = exp\{i\frac{\omega}{c}d \cdot (N\sigma_0 + \Delta N_{circ}\sigma_y + \Delta N_{lin}\sigma_z)\}, \tag{25}$$

where d is the sample thickness, N is the isotropic part of the complex refractive index, while ΔN_{lin} and ΔN_{circ} are contributions to the refractive index from linear and circular anisotropy for a thin sample, and σ_0 is the 2×2 unit matrix and σ_y, σ_z are Pauli matrices. After introducing $\Delta N = \sqrt{\Delta N_{lin}^2 + \Delta N_{circ}^2}$ the transmission matrix can be written in an equivalent form:

$$\hat{t}_{ij} = exp(i\frac{\omega}{c}Nd) \begin{bmatrix} cos(\frac{\omega}{c}\Delta Nd) + i\frac{\Delta N_{lin}}{\Delta N}sin(\frac{\omega}{c}\Delta Nd) & \frac{\Delta N_{circ}}{\Delta N}sin(\frac{\omega}{c}\Delta Nd) \\ -\frac{\Delta N_{circ}}{\Delta N}sin(\frac{\omega}{c}\Delta Nd) & cos(\frac{\omega}{c}\Delta Nd) - i\frac{\Delta N_{lin}}{\Delta N}sin(\frac{\omega}{c}\Delta Nd) \end{bmatrix} \tag{26}$$

When only one of the two polarization effects is present, one can reproduce the well-known forms

$$\hat{t}_{ij} = exp(i\frac{\omega}{c}Nd) \begin{bmatrix} exp(\frac{i\omega}{c}\Delta N_{lin}d) & 0 \\ 0 & exp(\frac{-i\omega}{c}\Delta N_{lin}d) \end{bmatrix}, \tag{27}$$

$$\hat{t}_{ij} = exp(i\frac{\omega}{c}Nd) \begin{bmatrix} cos(\frac{i\omega}{c}\Delta N_{circ}d) & sin(\frac{i\omega}{c}\Delta N_{circ}d) \\ -sin(\frac{i\omega}{c}\Delta N_{circ}d) & cos(\frac{i\omega}{c}\Delta N_{circ}d) \end{bmatrix}. \tag{28}$$

In the general case, the relative strength of the circular and linear anisotropy can be expressed by the elements of the transmission matrix according to $\frac{\Delta N_{circ}}{\Delta N_{lin}} = i\frac{\hat{t}_{xy}-\hat{t}_{yx}}{\hat{t}_{xx}-\hat{t}_{yy}}$. Figure S2 shows that circular and linear polarization effects are the same order of magnitude. This is highly remarkable, if we consider that some of the modes can only be excited by one of the two linear polarizations due to magnon selection rules. The two anisotropic contributions to the refractive index have the following forms:

$$\Delta N_{circ} = \frac{\hat{t}_{xy} - \hat{t}_{yx}}{\sqrt{(\hat{t}_{xy} - \hat{t}_{yx})^2 - (\hat{t}_{xx} - \hat{t}_{yy})^2}}arctg\left(\frac{\omega}{cd}\frac{\sqrt{(\hat{t}_{xy} - \hat{t}_{yx})^2 - (\hat{t}_{xx} - \hat{t}_{yy})^2}}{\hat{t}_{xx} + \hat{t}_{yy}}\right), \tag{29}$$

$$\Delta N_{lin} = -i\frac{\hat{t}_{xx} - \hat{t}_{yy}}{\sqrt{(\hat{t}_{xy} - \hat{t}_{yx})^2 - (\hat{t}_{xx} - \hat{t}_{yy})^2}}arctg\left(\frac{\omega}{cd}\frac{\sqrt{(\hat{t}_{xy} - \hat{t}_{yx})^2 - (\hat{t}_{xx} - \hat{t}_{yy})^2}}{\hat{t}_{xx} + \hat{t}_{yy}}\right). \tag{30}$$

The corresponding $\Delta N_{circ}(\omega)$ and $\Delta N_{lin}(\omega)$ spectra in the chiral phase of $Ba_2CoGe_2O_7$ are plotted in the and right left panel of Fig. S3, respectively. Our analysis shows that $\Delta N_{circ}(\omega)$ and $\Delta N_{lin}(\omega)$ are the same order of magnitude for the spin resonances and the rotation and ellipticity spectra evaluated as $\frac{\tan\theta + i\tan\eta}{1 - i\tan\theta\tan\eta} = \frac{\tilde{t}_{yx}}{\tilde{t}_{xx}}$ have dominant contributions from $\Delta N_{circ}(\omega)$.
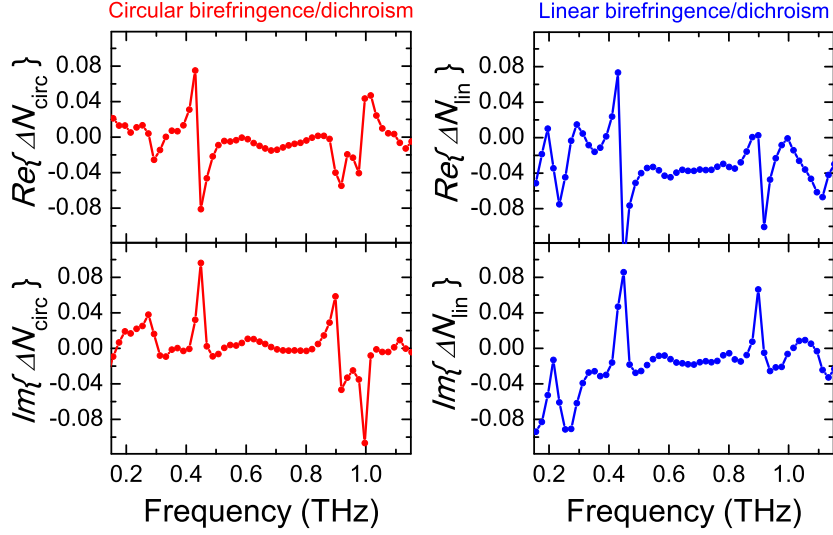

FIG. S3: | **Circular and linear birefringence/dichroism spectra in the field-induced chiral state of $Ba_2CoGe_2O_7$ with $B_{dc} = 7\,T$ parallel to [010].** The spectra in the left and right panel show the contributions to the refractive index from circular and linear polarization effects, respectively. Details of the evaluation are given in the text.

Besides the arguments above, the good correspondence between the calculated and experimental rotation/ellipticity spectra in Fig. S4 also implies that the diagonal components of the magnetoelectric tensor give main contributions to the polarization rotation and ellipticity. This fact is also manifested in the field-even nature of the polarization changes and the sign change of the polarization rotation and ellipticity upon the simultaneous rotation of $\mathbf{E}_\omega$ and $\mathbf{B}_{dc}$ around the [001] axis.
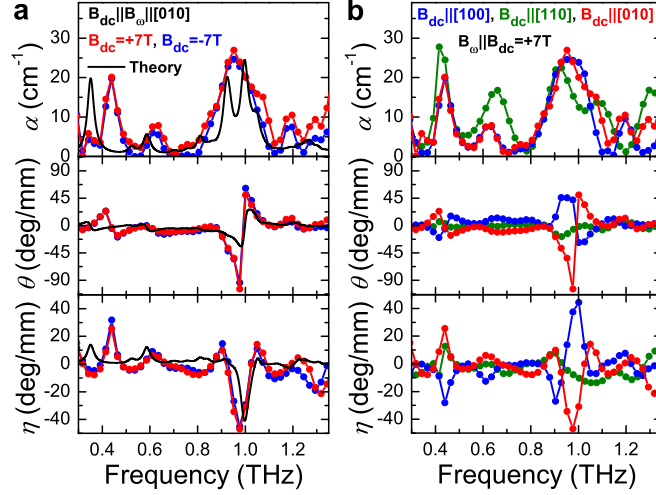
FIG. S4: | **Absorption (α), polarization rotation (θ) and ellipticity (η) spectra of the spin-wave modes** for light propagation along the [001] axis as measured by time-domain terahertz spectroscopy and calculated theoretically. Left panel: The polarization rotation and ellipticity are even function of the magnetic field. See good correspondence with spectra in the left panel of Fig. S2. Right panel: When the external magnetic field direction is rotated from [100] to [010] axis, both θ and η change sign, while they are zero within the experimental accuracy when the magnetic field points along [110] axis.

[1] Barron, L.D. *Molecular Light Scattering and Optical Activity*, (Cambridge University Press, Cambridge, 2004).

[2] Murakawa, H., Onose, Y., Miyahara, S., Furukawa, N. & Tokura, Y. Ferroelectricity Induced by Spin-Dependent Metal-Ligand Hybridization in $Ba_2CoGe_2O_7$. *Phys. Rev. Lett.* **103**, 137202 (2010).

[3] Miyahara, S. & Furukawa, N. Theory of magnetoelectric resonance in two-dimensional $S = 3/2$ antiferromagnet $Ba_2CoGe_2O_7$ via spin-dependent metal-ligand hybridization mechanism. *J. Phys. Soc. Jpn.* **80**, 073708 (2011).

[4] Landau, L.D., Lifshitz, E.M. & Pitaevskiî, L.P. *Electrodynamics of Continuous Media* (Pergamon Press Ltd, Oxford), 2nd ed., Chap. 101 and 104.

[5] Azzam, R.M.A. & Bashara, N.M. *Ellipsometry and polarized light* (North-Holland, Amsterdam) 1979.